Molecular Shuttles. A Computational Study (MM and MD) on the Translational Isomerism in Some [2]Rotaxanes

X. Grabuleda and C. Jaime*

Departament de Química, Universitat Autònoma de Barcelona. E−08193 Bellaterra (Barcelona), Spain

Received March 3, 1998

The translational isomerism experimentally observed in some [2]rotaxanes has been studied and modeled by means of molecular mechanics and molecular dynamics calculations using Allinger's MM3 force field and MM3*, the implemented version of MM3 for MacroModel. A reasonable agreement between the computed and experimental values for translational barriers has been obtained. Translational barriers are due to nonbonded interactions and can be tuned by introducing alkyl groups in the polyether chain.

Introduction

Chemists usually pursue the imitation of nature, which constructs large and complex systems by self-assembly processes with large degrees of efficiency.[1] Stoddart and co-workers have been working widely in this area[2] of supramolecular chemistry, exploiting the ideas of self-assembly[3−6] and self-replication[7] to construct large arrays from simple materials. One of the vehicles used for this research are rotaxanes (and polyrotaxanes), which are composed of one (or more) macrocycle(s) encircling a single dumbbell component[8] that bears two large blocking groups or stoppers at both ends of the linear thread. These stoppers serve to prevent the macrocycle from slipping off the end. The synthesis of such molecules has been carried out by different methods.[9−13] The interest in rotaxanes stems from the possibility that they might act as nanoscale switching devices. In these molecules, the macrocycle can shuttle back and forth along the thread in a new type of isomerism named translational isomerism.[14] The goals of Stoddart and co-workers are to achieve control over the shuttling processes and to design and synthesize new and improved rotaxanes.[15] Desymmetrization of the thread by insertion of two stations with different electronic properties produces [2]-rotaxanes, in which the position of the electron acceptor bead can be controlled by redox means. Following this idea, different types of [2]rotaxanes have been prepared by Stoddart's group,[16−19] four of which are studied in this article (compounds **1**−**4** in Scheme 1).

Computational methods can be a very useful tool for modeling molecular machines and molecular devices. In fact, articles exist in the literature that study the complexation of cyclobis(paraquat-*p*-phenylene), **5**, with different substrates, mainly through ab initio or semi-empirical calculations.[20−24] Molecular mechanics (MM) calculations readily allow energy minimizations and searching through large configurational spaces. The knowledge obtained from these theoretical studies can be useful in molecular nanotechnology to design and fabricate more powerful and useful molecular devices.[25,26] In this paper, molecular mechanics calculations have been applied to model the switching processes observed in [2]rotaxanes **1**−**4** (Scheme 1) where **5** is used as macrocycle.[27] MM3 was the selected force field[28] because,

(1) Whitesides, G. M.; Mathias, J. P.; Seto, C. T. *Science* **1991**, *254*, 1312.
(2) Philp, D.; Stoddart, J. F. *Angew. Chem., Int. Ed. Engl.* **1996**, *35*, 1154.
(3) Ashton, P. R.; Goodnow, T. T.; Kaifer, A. E.; Reddington, M. V.; Slawin, A. M. Z.; Spencer, N.; Stoddart, J. F.; Vicent, C.; Williams, D. J. *Angew. Chem., Int. Ed. Engl.* **1989**, *28*, 1396.
(4) Stoddart, J. F. In *Chirality in Drug Design and Synthesis*; Brown, C., Ed.; Academic: London, 1990; pp 53−81.
(5) Stoddart, J. F. In *Frontiers in Supramolecular Organic Chemistry and Photochemistry*; Schneider, H. J., Dürr, H., Eds.; VCH: Weinheim, 1990; pp 251−263.
(6) Stoddart, J. F. In *Host−Guest Molecular Interactions: from Chemistry to Biology*; Ciba Foundation Symposium 158; Wiley: Chichester, 1991; pp 5−22.
(7) Fouquey, C.; Lehn, J.-M.; Levelut, A.-M. *Adv. Mater.* **1990**, *2*, 254.
(8) Frisch, H. L.; Wasserman, E. *J. Am. Chem. Soc.* **1961**, *83*, 3789.
(9) Schill, G. In *Catenanes, Rotaxanes and Knots*; Academic Press: New York, 1971.
(10) Walba, D. M. *Tetrahedron* **1985**, *41*, 3167.
(11) Dietrich-Buchecker, C. O.; Sauvage, J. P. *Chem. Rev.* **1987**, *87*, 795.
(12) Stoddart, J. F. *Chem. Aust.* **1992**, *59*, 576.
(13) Wenz, G. *Angew. Chem., Int. Ed. Engl.* **1994**, *33*, 303.
(14) Schill, G.; Rissler, K.; Fritz, H.; Vetter, W. *Angew. Chem., Int. Ed. Engl.* **1981**, *20*, 187.
(15) Ballardini, R.; Balzani, V.; Credi, A.; Gandolfi, M. T.; Langford, S. J.; Menzer, S.; Prodi, L.; Stoddart, J. F.; Venturi, M.; Williams, D. J. *Angew. Chem., Int. Ed. Engl.* **1996**, *35*, 978.
(16) Ashton, P. R.; Bissell, R. A.; Spencer, N.; Stoddart, J. F.; Tolley, M. S. *Synlett* **1992**, 914.
(17) Ashton, P. R.; Bissell, R. A.; Górski, R.; Philp, D.; Spencer, N.; Stoddart, J. F.; Tolley, M. S. *Synlett* **1992**, 919.
(18) Ashton, P. R.; Bissell, R. A.; Spencer, N.; Stoddart, J. F.; Tolley, M. S. *Synlett* **1992**, 923.
(19) Bissell, R. A.; Córdova, E.; Kaifer, A. E.; Stoddart, J. F. *Nature* **1994**, *369*, 133.
(20) Castro, R.; Nixon, K. R.; Evanseck, J. D.; Kaifer, A. E. *J. Org. Chem.* **1996**, *61*, 7298.
(21) Castro, R.; Berardi, M. J.; Córdova, E.; Ochoa de Olza, M.; Kaifer, A. E.; Evanseck, J. D. *J. Am. Chem. Soc.* **1996**, *118*, 10257.
(22) Ballardini, R.; Balzani, V.; Credi, A.; Brown, C. L.; Gillard, R. E.; Montalti, M.; Philp, D.; Stoddart, J. F.; Venturi, M.; White, A. J. P.; Williams, B. J.; Williams, D. J. *J. Am. Chem. Soc.* **1997**, *119*, 12503.
(23) Castro, R.; Davidov, P. D.; Kumar, K. A.; Marchand, A. P.; Evanseck, J. D.; Kaifer, A. E. *J. Phys. Org. Chem.* **1997**, *10*, 369.
(24) Ricketts, H. G., Stoddart, J. F.; Hann, M. M. In *Computational Approaches in Supramolecular Chemistry*; Wipff, G., Ed.; Kluwer: Dordrecht, 1994; pp 377−390.
(25) Drexler, K. E. In *Engines of Creation*; Fourth Estate: London, 1990. (b) Drexler, K. E. In *Nanosystems: Molecular Machinery Manufacturing and Computation*; Wiley: New York, 1992. (c) *Molecular Electronic Devices*; Carter, F. L., Ed.; Dekker: New York, Vol. 1, 1982; Vol. 2, 1987.
(26) Fifth Foresight Conference on Molecular Nanotechnology, held November 5−8, 1997. http://www.foresight.org/Conferences/MNT05/Namo5.html.
(27) Brown, C. L.; Philp, D.; Stoddart, J. F. *Synlett* **1991**, 462.
(28) Allinger, N. L.; Yuh, Y. H.; Lii, J. H. *J. Am. Chem. Soc.* **1989**, *111*, 8551, 8566, and 8576.

10.1021/jo980400t CCC: $15.00
Published on Web 11/26/1998

Scheme 1

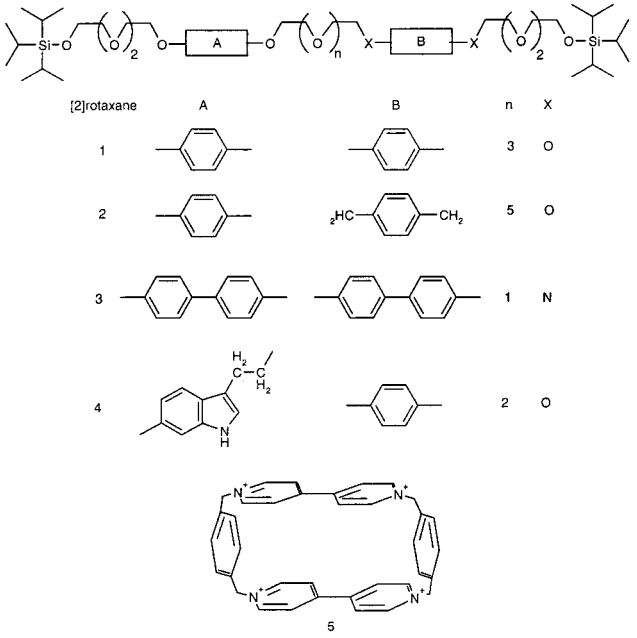

Table 1. Experimental Shuttling Barrier and Population Distribution for Translational Isomers As Obtained by DNMR

[2]rotaxane	$\Delta G^{\ddagger}$(A → B) kcal mol^{-1}	%A	%B
1	13.0[a]	50	50
2	13.7[b]	70[c]	30[c]
3		16	84[d]
4		100[e]	0[e]

[a] Approximate value obtained from different ^{1}H NMR probes (see ref 43 for more details). [b] Average value obtained from two different ^{1}H NMR probes at 253 K (see ref 16 for more details). [c] From its ^{1}H NMR spectrum at 233 K (see ref 19). [d] From ^{1}H NMR studies at 229 K (see ref 22). [e] From ^{1}H NMR studies at 233 K (see ref 31).

according to our own experience,[29] it behaves reasonably well when studying interactions between nonbonded molecules. All studied linear components contain two stations (sites on which the macrocycle can be found). Table 1 contains data experimentally obtained by dynamic ^{1}H NMR spectroscopy for **1**−**4**. The final aim of this article is to reproduce these experimental data to find the interactions involved in the shuttling process and to obtain information for controlling the macrocycle switching.

Computational Details. MM computations were carried out by using either the original MM3 force field or its MacroModel version (MM3*). Allinger's MM3(92)[30] force field[28] calculations were performed on a VAX

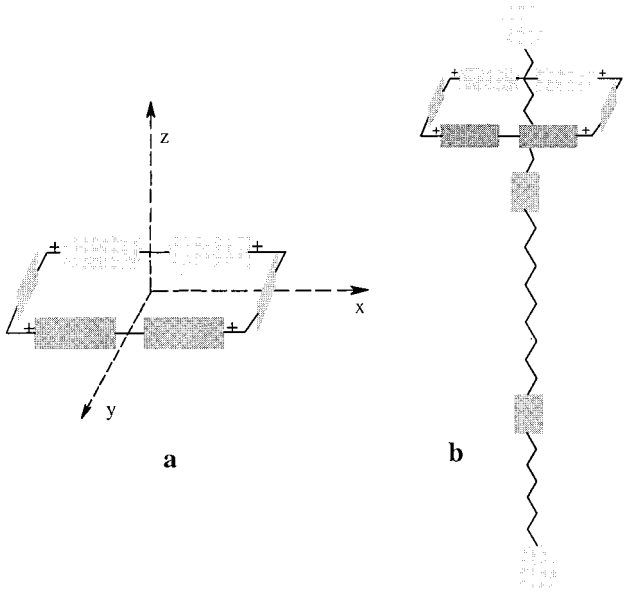

Figure 1. (a) Orientation used for the cyclobis(paraquat-*p*-phenylene) tetracationic macrocyle. (b) Schematic representation of the finally oriented molecular structure of a [2]rotaxane.

ALPHA-2100-4/275 computer at the Computer Center of the Universitat Autònoma de Barcelona. Unless otherwise noted, all optimizations were carried out with the default options (block-diagonal algorithm and in a vacuum). MM3* calculations were performed on a Silicon Graphics INDY computer with R4600PC processor using Still's MacroModel 4.0 molecular modeling package.[31] The conjugate gradient minimization algorithm (PRCG)[32] from E. Polak and G. Ribiere was used with this force field, allowing enough cycles to ensure convergence. The GB/SA solvation model[33] was used when modeling solvent effects under MacroModel.

Preliminary molecular dynamics (MD) calculations[34] were also performed using MacroModel and BatchMin 5.0 molecular modeling programs. MD simulations were run exclusively for the [2]rotaxane **1**. The dumbbell component provided restraint at selected positions by fixing the distances between the sp^3 carbon atoms of the cyclophane and one of the atoms located inside the macrocyclic cavity. The region studied spans the range from 0 to 16 Å with steps of 1.0 Å (see Figure 2) due to the symmetric nature of **1**. The selected restraints allow the dumbbell component to adopt any conformation for the polyether chain, and the aromatic station not included in the cavity can approach any of the paraquat residues. Also, the two components (macrocycle and dumbbell) can redirect one to the other. The present model covers larger parts of the configurational space of the [2]rotaxane than the MM model. Simulations using the MM3* force field were carried out in a vacuum with a distance-dependent dielectric electrostatics treatment. Extended nonbonded cutoff distances were set to 8.0 Å for the van der Waals interactions and 20.0 Å for the electrostatic interactions. Interatomic distances re-

(29) (a) Jaime, C.; Redondo, J.; Sánchez-Ferrando, F.; Virgili, A. *J. Org. Chem.* **1990**, *55*, 4773. (b) Redondo, J.; Jaime, C.; Virgili, A.; Sánchez-Ferrando, F. *J. Mol. Struct.* **1991**, *248*, 317. (c) Fotiadu, F.; Fathallah, M.; Jaime, C. *J. Inclusion Phenom.* **1993**, *16*, 55. (d) Fathallah, M.; Fotiadu, F.; Jaime, C. *J. Org. Chem.* **1994**, *59*, 1288. (e) Pérez, F.; Jaime, C.; Sánchez-Ruiz, X. *J. Org. Chem.* **1995**, *60*, 3840. (f) Ivanov, P. M.; Jaime, C. *Anales de Quím., Int. Ed.* **1996**, *92*, 13. (g) Ivanov, P. M.; Jaime, C. *J. Mol. Struct.* **1996**, *377*, 137. (h) Salvatierra, D.; Ivanov, P. M.; Jaime, C. *J. Org. Chem.* **1996**, *61*, 7012. (i) Salvatierra, D.; Jaime, C.; Virgili, A.; Sánchez-Ferrando, F. *J. Org. Chem.* **1996**, *61*, 9578. (j) Entrena, A.; Jaime, C. *J. Org. Chem.* **1997**, *62*, 5923. (k) Cervelló, E.; Jaime, C. *THEOCHEM* **1998**, *428*, 195. (l) Sánchez-Ruiz, X.; Ramos, M.; Jaime, C. *J. Mol. Struct.* **1998**, *442*, 93. (m) Cervelló, E.; Jaime, C. *Anales de Quím., Int. Ed.* **1998**, *00*, 0000.

(30) Version 92 available at Technical Utilization Corporation, 235 Glen Village Court, Powell, OH 43065.

(31) Mohamdai, F.; Richards, N. G. J.; Guida, W. C.; Liskamp, R.; Caufield, C.; Chang, G.; Hendrickson, T.; Still, W. C. *J. Comput. Chem.* **1990**, *11*, 440.

(32) Polak, E.; Ribiere, G. *Rev. Fr. Inf. Rech. Oper.* **1969**, *16*, 35.

(33) Still, W. C.; Tempczyk, A.; Hawley, R. C.; Hendrickson, T. *J. Am. Chem. Soc.* **1990**, *112*, 6127.

(34) More work on this topic is in progress in our laboratories.

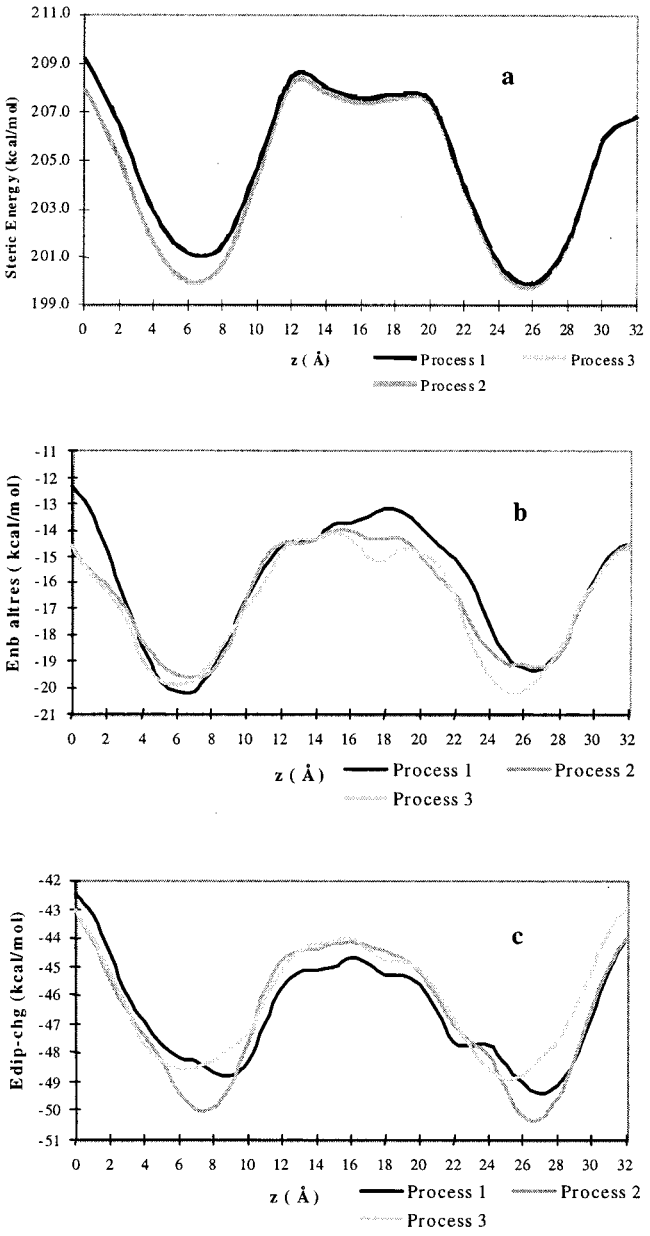

Figure 2. (a) Changes in the steric energy during the translational isomerism process for [2]rotaxane **1** as obtained by MM3* calculations. (b)−(c) Variation of the van der Waals and dipole-charge energy terms during the translational isomerism process for [2]rotaxane **1** as obtained by MM3 calculations.

straints were imposed using a flat-bottom function with deviations of 0.1 Å. Obtained geometries of **1** were optimized at each point by the Polak−Ribiere conjugate gradient method, allowing 5000 iterations with the three-point line searcher activated, before starting the MD simulations. All MD runs were started with an initial temperature of 5 K, thus initializing the atomic velocities, which together with the MM optimized coordinates determine the point in the phase space at which the preparation of the system for the simulations starts. Four consecutive MDYN commands were executed in all cases. These commands warm the system from 50 to 250 K at 1 ps intervals. Then, a 10 ps simulation follows to bring the system up to 298 K. Finally, a 2500 ps simulation at a constant temperature of 298 K was run with a 1 fs time step and application of the SHAKE algorithm to the stretching interactions.

Scheme 2

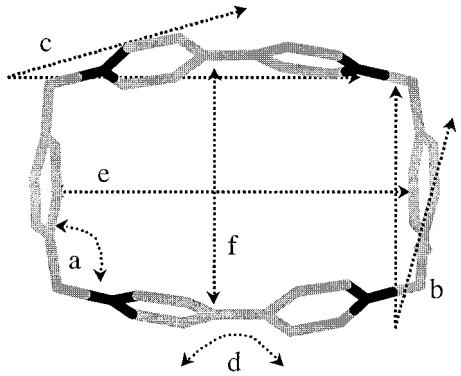

Modeling of the Components. One unit of cyclobis(paraquat-*p*-phenylene) was constructed using standard bond lengths and angles. Semiempirical calculations using MOPAC-93[35] under the PM3 method[36] without geometry optimization were used to determine the charge distribution for the cyclophane. Charges were introduced as parameters in the MM3(92) calculations.[37] The MM3 force field does not contain any atom type corresponding to a pyridinium nitrogen; most of its parameters were taken from those for an sp^2 nitrogen (atom type 40), but some were taken from those for sp^2 carbon. During the realization of this work, the first parametrization for positively charged conjugated nitrogen-containing compounds for MM2(91) and MM3(94) force fields appeared in the literature.[38] Nevertheless, the required parameters to model the cyclophane are not available.[39] MM3(92) also does not contain any parameter for the Si−O stretching. The stretching constant for the C−O bond of the MM3 force field was used to model the Si−O interaction, with modification of the C−O bond length to 1.6 Å.[40] The role played by the stoppers in the translational isomerism (only steric hindrance) led us to this assumption. Parameters for the new positively charged pyridinium nitrogens for the MM3* force field were considered equal to those for the already existing nitro atom type. Stretching parameters for N(nitro)−C(aromatic) were considered to be equal to those for N(nitro)−C(aliphatic) due to the electrostatic treatment of MacroModel, which uses charges generated from bond dipoles. The tetracationic cyclophane was fully minimized, and good agreement with X-ray structures was obtained (Scheme 2 and Table 2). The linear components were also fully minimized, assuming an antiperiplanar conformation in all of the polyether chains.

Translational Isomerism Emulation. The tetracationic macrocycle was oriented by placing one positive nitrogen onto the *XY* plane and the geometrical center of the cavity at the center of the coordinate system (Figure 1a). The linear component was oriented along the *Z* axis, with the geometrical center of one of the two

(35) Stewart, J. J. P. Fujitsu Limited: Tokyo, Japan, 1993.
(36) Stewart, J. J. P. *J. Comput. Chem.* **1989**, *10*, 209 and 221.
(37) Standard deviation between the computed charge distribution for its X-ray structure and the one used in the calculations was evaluated to be $\sigma = \pm 0.018$.
(38) McGaughey, G. B.; Stewart, E. L.; Bowen, J. P. *J. Comput. Chem.* **1996**, *17*, 1395.
(39) More work on this aspect is being carried out in our laboratories.
(40) *DTMM (Desktop Molecular Modeling)*, Oxford Electronic Publishing, Oxford University Press: Walton Street, Oxford OX2 6DP, U.K.

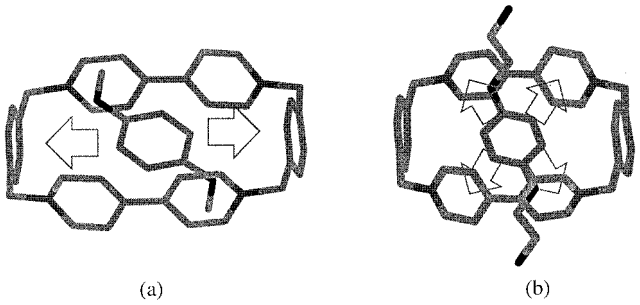

Figure 3. Fragments of minima structure for [2]rotaxane **1** showing the π stacking and "T-type" edge-to-face interactions: (a) obtained by MM3 and (b) obtained by MM3*.

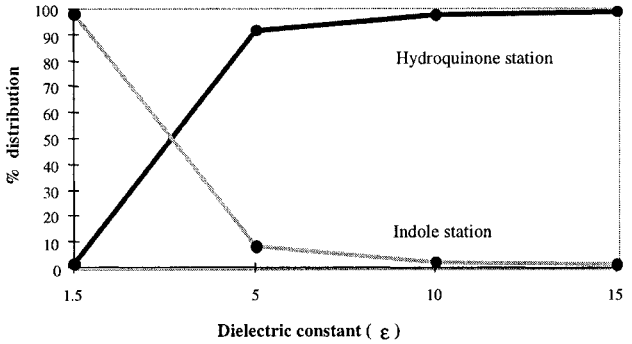

Figure 4. Variation of the localization of the macrocycle with dielectric constant in MM3 calculations for [2]rotaxane **4**.

Table 2. Experimental (X-ray) and Computed (MM3 and MM3*) Structural Parameters for the Cyclobis(paraquat-*p*-phenylene) Unit

	X-ray	MM3	MM3*
a	108.5°	110.4°	106.5°
b	14.0°	6.1°	4.7°
c	23.0°	14.3°	11.9°
d	19.0°	13.6°	−3.1°
e	10.3 Å	10.3 Å	10.5 Å
f	6.8 Å	7.5 Å	7.1 Å

Table 3. Computed Occupancy of the Translational Isomers for [2]Rotaxanes 2 and 3 using Different Values for the Dielectric Constants (ϵ) Obtained from MM3 Calculations at 298 K

	$\epsilon = 1.5$	$\epsilon = 5$	$\epsilon = 10$	$\epsilon = 15$
		hydroquinone: *p*-xylyl		
2	72:28	100:0	99.7:0.3	92.6:7.3
		benzidine : biphenol		
3	98:2	100:0	99.9:0.1	94.6:5.4

aromatic rings slightly beneath the center of the coordinate system. Merging these two independent sets of coordinates into one single assembly produced the molecular structure. The aromatic stations of the dumbbell were always parallel to the paraquat units of the macrocycle (Figure 1b). The molecule was optimized under both force fields, and the translational isomerism of the cyclophane between the stations was emulated by modifying the *z* coordinates of the dumbbell at 1 Å steps. This strategy moves the other station toward the cavity of the macrocycle. Some reference atoms were restrained in each step to ensure the initial orientation, and the energy was minimized. Three of the C(sp^3) of the macrocycle were forced to stay in the *XY* plane, and one of the C_{ipso} in the linear component was forced to be in the *Z* axis. The switching process was repeated two more times (going back and forth) to guarantee a uniform and single phenomenon and to release tensions from the system. The graphical representation of energy changes involved in the translational isomerism produced curves with two energy minima corresponding to the inclusion of the stations inside the cyclophane cavity. Figure 2a represents the energy variation for [2]rotaxane **2** in MM3* calculations as an example. Those preliminary energy minima were reoptimized by removing all restraints and producing the final energy minimum.

This methodology chosen to model the translational isomerism ignores three important interactions present in the [2]rotaxanes: (i) the [C−H·····O] hydrogen bonding between some acidic H atoms in the pyridinium unit and the appropriate O atoms in the polyether, (ii) the lateral $\pi-\pi$ stacking interactions involving the aromatic rings not included inside the cyclophane, and (iii) the gauche effect present in the $-OCH_2CH_2O-$ units of the polyether component. All of these can be ignored as a first approximation. Presumably, the [C−H·····O] interactions are present wherever the cyclophane is located; therefore, they will add the same stabilization to the system and its effect can be ignored. Lateral $\pi-\pi$ stacking interactions can be present at energy minima, creating an extra stabilization not considered in these computations. Computed energy barriers should thus be underestimated by a few kcal mol^{-1}. Finally, although the gauche effect will definitely affect the general molecular shape (especially for the dumbbell component), we have considered the molecule to exist "in average" in an all-trans conformation. Ulterior results from molecular dynamics simulations have reinforced this supposition (see below).

Results

Cyclobis(paraquat-*p*-phenylene). This tetracationic unit, **5** (Scheme 1), incorporates two π-electron-deficient paraquat residues connected in a phanelike manner by means of two *para*-phenylene groups, and it can act as a host for face-to-face complexation. X-ray structural analysis[41,42] showed that the macrocycle adopts a centrosymmetric rectangular boxlike conformation with the two paraquat units forming the longer sides and the two *para*-xylylene residues forming the shorter ones. There is a twist angle (19°) between the two positively charged pyridine rings of each paraquat unit, and in addition, there are deformations of both the paraquat and *para*-xylylene components, producing a bowing of the cyclophane sides. The overall dimensions of the macrocycle are 10.3 Å between the centroids of the two *para*-phenylene rings and 6.8 Å between the carbon atoms in position 4 of the pyridinium rings of different paraquat units. The results obtained by MM3 and MM3* were in reasonable agreement with the experimental ones. The numerical values of the main characteristics are given in Table 2. MM3 gives the more accurate approach to the X-ray cyclophane structure, whereas MM3* strongly disagrees in the twist angle of the pyridinium units. All the calculations were carried out for isolated tetracations.

[2]Rotaxane 1. The linear component of **1** presents two identical stations in the form of hydroquinone units

(41) Allwood, B. L.; Spencer, N.; Shahriari-Zavareh, H.; Stoddart, J. F.; Williams, D. J. *J. Chem. Soc., Chem. Commun.* **1987**, 1064.
(42) Stoddart, J. F. *Pure Appl. Chem.* **1988**, *60*, 467.

Table 4. Aromatic Station Occupied by Tetracationic Macrocycle in MM3* Calculations in Vacuum and using the GB/SA Solvation Model Compared with Experimental Results for [2]Rotaxanes 2−4

[2]rotaxane	MM3*			
	vacuum	H_2O	$CHCl_3$	experimental
2	*p*-xylyl	hydroquinone	hydroquinone	hydroquinone
3	benzidine	biphenol	benzidine	benzidine
4	hydroquinone	hydroquinone	hydroquinone	hydroquinone

Scheme 3

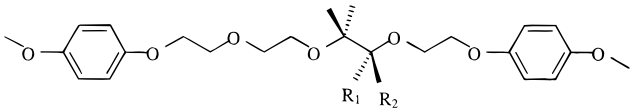

[2]rotaxane	Substituents	Shuttling barrier
1a	$R_1 = R_2 = H$	20.7 kcal mol^{-1}
1b	$R_1 = CH_3$, $R_2 = H$	21.5 kcal mol^{-1}
1c	$R_1 = R_2 = CH_3$	32.3 kcal mol^{-1}

Table 5. Averaged Energy (kcal mol^{-1}) Increments for Significant Energy Terms between Maxima and Minima Structures in the Three Simulation Processes of [2]Rotaxanes 1, 1a, 1b, and 1c

Δ	**1**	**1a**	**1b**	**1c**
stretching	0.3	1.7	2.4	3.5
bending	−0.1	1.2	1.1	1.3
torsion	−0.1	−0.4	−0.5	−0.2
van der Waals	5.6	9.4	10.3	16.9
(1−4)interactions	0.6	9.0	8.6	12.1
dipole−charge	5.1	5.4	5.4	4.7
dipole−dipole	−0.1	−1.5	−1.7	−0.8
charge−charge	−0.6	−4.2	−4.3	−6.0

Table 6. Structural Parameters for the Cyclobis(paraquat-*p*-phenylene) Macrocycle of [2]Rotaxane 1 and Modified [2]Rotaxanes 1a, 1b, and 1c As Obtained by MM3 Calculations

	1	**1a**	**1b**	**1c**
a	110.0°	113.9°	114.9°	115.6°
b	4.2°	5.9°	4.1°	1.3°
c	15.0°	25.2°	25.0°	26.5°
d	6.7°	−7.2°	−7.7°	−12.0°
e	10.1 Å	9.6 Å	9.7 Å	9.5 Å
f	7.6 Å	8.8 Å	8.7 Å	9.0 Å

grafted symmetrically onto the polyether chain. The cyclophane moves back and forth between the two stations, as demonstrated from the temperature dependence of its ^{1}H NMR spectra,[43] which afforded $\Delta G^{\ddagger}$ values of ca. 13 kcal mol^{-1} for the degenerated process (see Table 1). As expected, the process emulation showed two energy minima with a Bolztmann distribution (at 298 K) of 50% for each when the MM3 force field was used. The energy barrier for the shuttling was computed to be 10.8 kcal mol^{-1}. Dipole-charge and van der Waals interactions were the most important energy terms controlling the process. Graphical representation of these energy terms roughly produced the profile of the inclusion process (Figures 2b,c). No substantial change of the tetracationic macrocycle geometry was detected when the hydroquinone units were inside its cavity, in agreement with experiments.[43] The distance between paraquat units decreased slightly (from 7.5 to 7.3 Å) because of the π stacking acceptor−donor interactions.[44] The presence of "T-type" edge-to-face interactions[45] involving some of the hydrogens of the hydroquinone rings and the *p*-phenylene units of the cyclophane were also detected (Figure 3a).

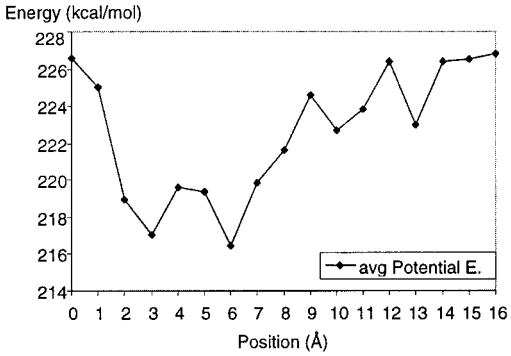

Figure 5. Average potential energy versus position of the dumbbell component of [2]rotaxane **1** as obtained in the 240 samplings belonging to the last 300 ps of the MD simulation.

Similar but not identical results were found when using the MM3* force field. Two degenerate energy minima were obtained and the energy barrier for the shuttling process was computed to be 11.0 kcal mol^{-1}. The van der Waals and electrostatic terms were again those mainly controlling the shuttling. The geometry of the cyclophane was also modified by the presence of the hydroquinone units that tried to maximize the π stacking and the edge-to-face interactions (Figure 3b).

[2]Rotaxane 2. The replacement of one of the two hydroquinone rings in [2]rotaxane **1** by one unit of lower π-donating ability should permit the control of the positioning of the tetracationic macrocycle.[17] In [2]-rotaxane **2**, one hydroquinone was replaced by one *p*-xylyl residue and the preferential occupation of the hydroquinone site (π-electron richer) was expected. However, analysis of the ^{1}H NMR spectrum at 233 K revealed that the macrocycle distributed itself between both sites with a 70/30 occupancy at the hydroquinone/*p*-xylyl residues. Computer line-shape analysis gave $\Delta G^{\ddagger}$ values of 13.7 kcal mol^{-1} at 253 K for the conversion of the major isomer to the minor isomer and 13.5 kcal mol^{-1} for the opposite process.[16]

MM3 calculations predicted an occupancy of 72/28 (at 25 °C) for the hydroquinone/*p*-xylyl residues, and the computed barrier of shuttling was 11.4 kcal mol^{-1} for the conversion of the major into the minor isomer, in total agreement with experiments. Again, the van der Waals and dipole-charge terms were responsible for these energy minima, with the first prevailing over the second and stabilizing the hydroquinone site occupancy. The relative orientation of the two stations of the linear component is noteworthy. The *p*-xylyl residue was

(43) Anelli, P. L.; Spencer, N.; Stoddart, J. F. *J. Am. Chem. Soc.* **1991**, *113*, 5131.

(44) Hunter, C. A.; Sanders, J. K. M. *J. Am. Chem. Soc.* **1990**, *112*, 5525.

(45) Jorgensen, W. L.; Severance, D. L. *J. Am. Chem. Soc.* **1990**, *112*, 4768.

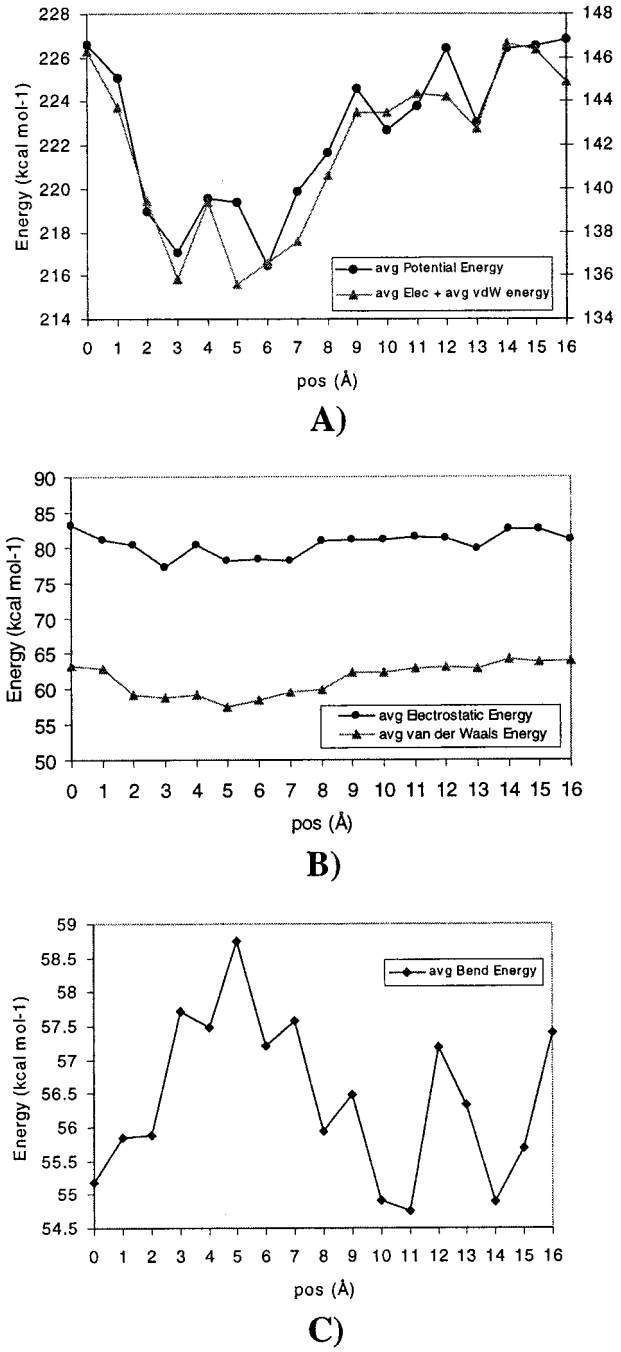

Figure 6. Energy distribution versus position of the dumbbell component of [2]rotaxane **1** as obtained in the MD simulations: (A) total energy (right axis) and the sum of electrostatic and van der Waals contributions (left axis), (B) electrostatic and van der Waals contributions, and (C) bending contribution.

computed to be perpendicular to the hydroquinone and paraquat units when not included, but it was observed to be parallel when entering the cyclophane cavity. The gradual modification of the torsion angles of the polyether chain was accompanied by a variation of the cyclophane geometry, converting a boxlike shape into a trapezoidal boxlike shape with distortion of the *p*-phenylene groups.

The emulation using the MM3* force field showed a stabilization of the hydroquinone site with respect to the *p*-xylyl residue. The analysis of the energy terms showed that although van der Waals interactions favored the hydroquinone site, the electrostatic interactions gave lower energy values for the *p*-xylyl site—it was the contribution of the bending and torsion energy terms which made the hydroquinone site the more stable. However, after reoptimizing the minima structures for the MM3* calculations, without restraints over the reference atoms, the relative stability was inverted. These results do not agree with the experimental data. Here the electrostatic term clearly dominates; the van der Waals term afforded an energy gap of 0.6 kcal mol^{-1} stabilizing the hydroquinone site, and the electrostatic term stabilized the *p*-xylyl site by 1.5 kcal mol^{-1}. On the contrary, the results from MM3 calculations showed that contribution of the electrostatic term was unimportant and the quantitative differences generated by this term were not significant.

[2]Rotaxane 3. The two stations used for **3** are based on 4,4′-disubstituted biphenyl derivatives, benzidine and 4,4′-biphenol. They differ in their redox properties, as benzidine is much more easily oxidized than 4,4′ -biphenol. Previous complexation studies[46] of these biphenyl guests with cyclobis(paraquat-*p*-phenylene) demonstrated that the complexation constant with benzidine was 10 times greater than the complexation constant with 4,4′-biphenol. This [2]rotaxane presents a thermal equilibrium with a ratio of 84/16 for the benzidine/biphenol occupation (at 229 K) as deduced from NMR spectroscopy.[19]

MM3 calculations indicated the presence of two energy minima, with the one corresponding to the inclusion of the benzidine unit being more stable. These results were only in qualitative agreement with experiments (the ratio based on a Boltzmann distribution at 298 K was 98/2). The computed energy barrier for the conversion of the major to the minor isomer was found to be 15.5 kcal mol^{-1}. Lack of the corresponding experimental value prevents comparison. The dipole-charge energy term was governing the formation and stabilization of the minima.

When the benzidine residue is inside the cyclophane, the computed geometry agrees with that proposed by Stoddart and determined by NOE experiments in the complexation with isolated stations.[46] Favorable π stacking interactions leading to a decrease of the internal distance between paraquat units were observed. When the biphenol ring is included, the computed geometry (the two aromatic rings of biphenol were equally distributed inside the cavity) differed from that experimentally deduced from NOE experiments (where only one ring was complexed).

The MM3* force field gave two sets of minima structures differing by 3 kcal mol^{-1}, with the inclusion of the benzidine unit being the more stable. This energy gap caused the benzidine site to be occupied almost exclusively (99.6%). The energy barrier for the shuttling between stations was computed to be 11.4 kcal mol^{-1}.

[2]Rotaxane 4. The stations for [2]rotaxane **4** were one hydroquinone ring and one 2,3,5-trisubstituted indole. The high π-electron-rich nature of indole would force the preferential occupation of this station; moreover, its oxidation should result in the jump of the macrocycle to the hydroquinone station. The ^{1}H NMR spectroscopy revealed that the macrocycle was indeed located exclusively at the hydroquinone site.[18] This result was originally interpreted as a reflection of the conflict between steric (indole ≫ hydroquinone) and electronic (indole >

(46) Córdova, E.; Bissell, R. A.; Spencer, N.; Ashton, P. R.; Stoddart, J. F.; Kaifer, A. E. *J. Org. Chem.* **1993**, *58*, 6550.

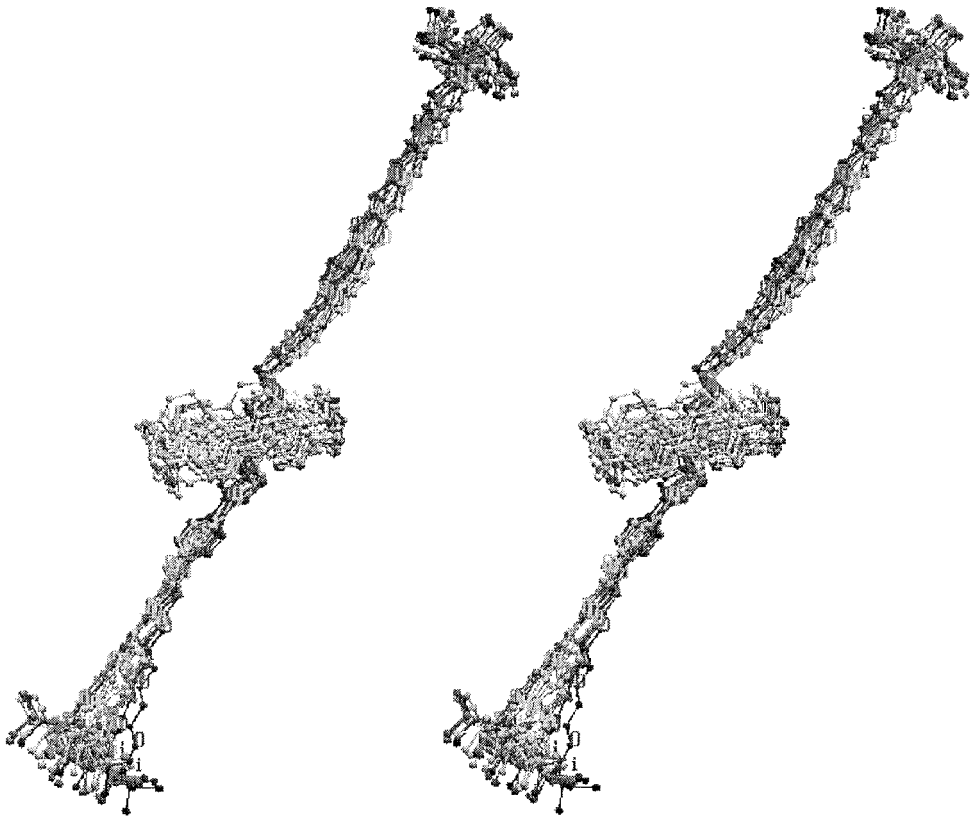

Figure 7. Stereoview of the MD samplings corresponding to the local minimum of [2]rotaxane **1** at the shuttling position 13 Å.

hydroquinone) demands within the system, as reported[17] for a [2]catenane in other previous works.

The structural characteristics of this [2]rotaxane make it difficult to emulate the switching process. The MM3 computed energies for energy minima indicated an exclusive occupancy of the indole station, in clear disagreement with experimental results. The computed energy difference between the two translational isomers was 2.2 kcal mol^{-1}.

Modeling of Solvent Effects. Considering that molecular mechanics and, specifically, the MM3 force field have allowed the correct modeling of the behavior of most of the studied [2]rotaxanes, one might think that interactions other than a purely steric control may participate in [2]rotaxane **4**, important enough to modify the relative stability of the stations. The effect of solvent was neglected in our calculations. Unfortunately, MM3 does not contain any solvation model, but it is possible to indirectly simulate the global effect of the solvent by changing the dielectric constant value. The energy minima were computed again using dielectric constant values of 5, 10, and 15 to simulate the solvent used experimentally (CH_3CN). Figure 4 graphically shows the changes in population produced by the dielectric constant variation: inversion of the relative stability. The same changes in the dielectric constant value were also done for the other previously studied [2]rotaxanes (**1**−**3**). The newly computed results kept the same relative stability order between the stations in all the [2]rotaxanes, but an increase in the computed occupancy of the translational isomers was observed. Table 3 shows this behavior for [2]rotaxanes **2** and **3**.

Computations (MM3*) and experiments[18] present a good agreement in the preferred station for [2]rotaxane **4** (hydroquinone). Most of the NMR experiments were carried out in CD_3CN as solvent. Although some computer models for this solvent have been described in the literature,[47,48] they are not implemented in standard packages yet. Nevertheless, the continuum solvation model (GB/SA)[33] available in MacroModel was used in our calculations. $CHCl_3$ and H_2O were simulated, and the results indicated an increase in the energy difference between energy minima. To keep the parallelism with the MM3 calculations, new optimizations for all other energy minima structures of [2]rotaxanes **2** and **3** were undertaken considering these solvation models (Table 4). Only in the case of [2]rotaxane **4** do the calculations always agree with the experimental results. Moreover, only $CHCl_3$ solvent calculations can reproduce the experimental results for [2]rotaxanes **2**−**4**, although acetonitrile should behave more similarly to water than to chloroform.

The energetic results from the MM calculations with MM3 and MM3* force fields differ significantly, especially when the solvent influence is considered. Although MM3 behaves in a predictable way, MM3* behaves erratically. The parametrization used in this work for dealing with this highly charged species is provisional, and it is likely to be the reason for the large discrepancies observed. The absence of suitable parameters for the pyridinium N atom in MM3 forced us to compute atomic charges by a semiempirical molecular orbital method and to use them within the frame of MM3. Moreover, the impossibility of introducing individual atomic charges in MacroModel required the use of some of the already existing atom types within the parameters set (i.e., nitro instead of pyridinium).

(47) Jorgensen, W. L.; Briggs, J. M. *Mol. Phys.* **1988**, *63*, 547.
(48) Cabaleiro-Lago, E. M.; Rios, M. A. *J. Phys. Chem. A* **1997**, *101*, 8327.

Tuning of the Shuttling Barrier. The effect on the energy barrier of the introduction of some substituents anchored in the central zone of the polyether chain has also been explored. This modification may increase the energy values for the shuttling process, and the macrocycle will only switch when external stimuli (oxidization of the aromatic station) are made and not at thermal equilibrium. We have been working in this direction, and preliminary results are quite satisfactory. We have repeated the emulation processes for the [2]rotaxane **1**, introducing different steric hindrances. Linear components were modified by adding from two to four methyl substituents around the central zone of the polyether chain. A generalized structure showing the methyl substituents introduced in the linear component and the MM3 computed steric energy for the barrier of switching are depicted in Scheme 3. The energy profiles obtained from the three switching processes indicate that the shuttling barrier is always larger than the 10.8 kcal mol^{-1} obtained for the [2]rotaxane **1**. From detailed analysis of the energy terms (Table 5), it can be deduced that the addition of methyl groups in the polyether chain affects the shuttling process in two ways: van der Waals and torsion terms act to prevent the translational isomerism, but electrostatic and dipole−dipole terms favor the process. The deformations observed in maxima energy structures for [2]rotaxanes **1a**, **1b**, and **1c** are mainly located in the geometry of cyclobis(paraquat-*p*-phenylene). These deformations come from the region of the methylene unit that joins the paraquat and *p*-phenylene fragments and are shown in Table 6.

Molecular Dynamics Simulations on the Shuttling of [2]Rotaxane 1. To gain more information of the interactions involved in the translational isomerism of these [2]rotaxanes and to avoid the limitations of molecular mechanics (MM) calculations, a preliminary study of [2]rotaxane **1** was carried out using molecular dynamics (MD) simulations. The rigidity of the polyether chain used in MM calculations might prevent important interactions from being considered in a minimization approach (see Translational Isomerism Emulation). MD calculations allow extensive sampling of the conformational phase space and therefore more readily permit observation and evaluation of such previously mentioned interactions.

Results from the MD simulations on **1** are graphically presented in Figure 5, and they illustrate the variation of the average potential energy (240 samplings within the last 300 ps) with the distance between the macrocycle and the dumbbell. Simulations were run without interatomic distance constraints for the zone between 2 and 7 Å, where the aromatic station lies under the influence of the macrocycle, to find the global energy minimum from different starting points. The shuttling barrier can be evaluated to be about 10.5 kcal/mol, a value that is very near to that obtained by our MM calculations (11 kcal/mol for **1**, see above). Figures 6A and 6B show that the van der Waals and electrostaic contributions to the total energy are what mainly control this process and locates the minimum at the 5 Å position. Nevertheless, the position of the final energy minimum is tuned by the bending contribution (Figure 6C). The presence of the hydroquinone unit inside the macrocycle cavity (the zone between 3 and 7 Å) produces large deformations in the bond angles.

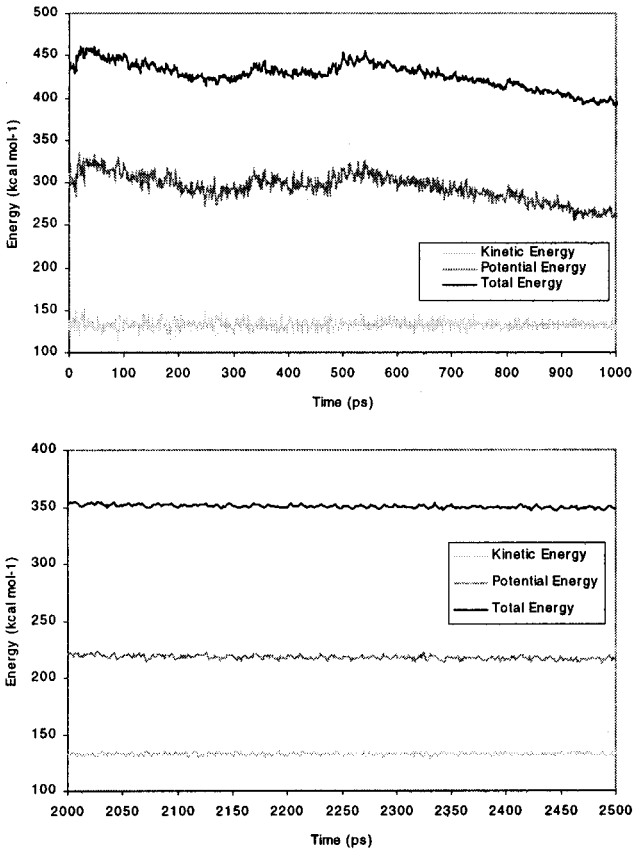

Figure 8. Variation of the potential, kinetic, and total energies for the MD simulations of the shuttling process of [2]rotaxane **1** in position 6 Å.

In contrast to the MM calculations, MD simulations show the presence of low-energy zones on the shuttling process different from the energy minima (see point 13 in Figure 5). The analysis of the MD samplings indicate the presence of stabilizing interactions of the type of [C−H·····O] hydrogen bonds between acidic protons of the pyridinium rings and O atoms of the polyether chain located at proper distances (2.6−2.8 Å). Clearly, these interactions are due to the conformational changes produced by the gauche effect over the $-OCH_2CH_2O-$ torsion angles that were not considered in the MM calculations. Figure 7 shows the stereoview of the MD samplings for position 13. It is clear that there exist two such interactions, one at each side of the macrocycle. Analysis of the MD samplings for position 12, which is more energetic than 13, shows that only one hydrogen bond interaction between the macrocycle and the polyether chain is present. Those oxygen atoms nearer to the macrocycle are those modifying the all-anti conformation. These stabilizing interactions have also been observed in the two positions corresponding to the energy minima (3 and 6 Å, see Figure 5).

It is worth mentioning here that all the MD simulations of this work present a characteristic trend regarding the evolution of energy during the 2500 ps simulation (Figure 8). The potential energy oscillates significantly in the zone of 0−1000 ps, and it is there where several structures presenting lateral $\pi-\pi$ stacking interactions between the macrocycle and the hydroquinone rings can be detected (Figure 9). After about 1000 ps in the trajectory, the energy starts to stabilize, and when the simulation arrives at about the 2000 ps mark, the system

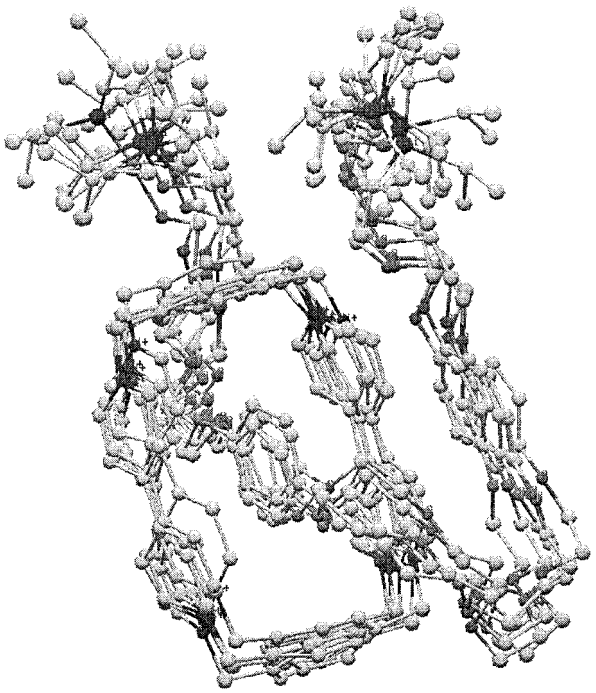

Figure 9. Superimposition of structures obtained in the first 1000 ps of the MD trajectory of [2]rotaxane **1** at position 3 Å showing the alongside $\pi-\pi$ stacking interactions.

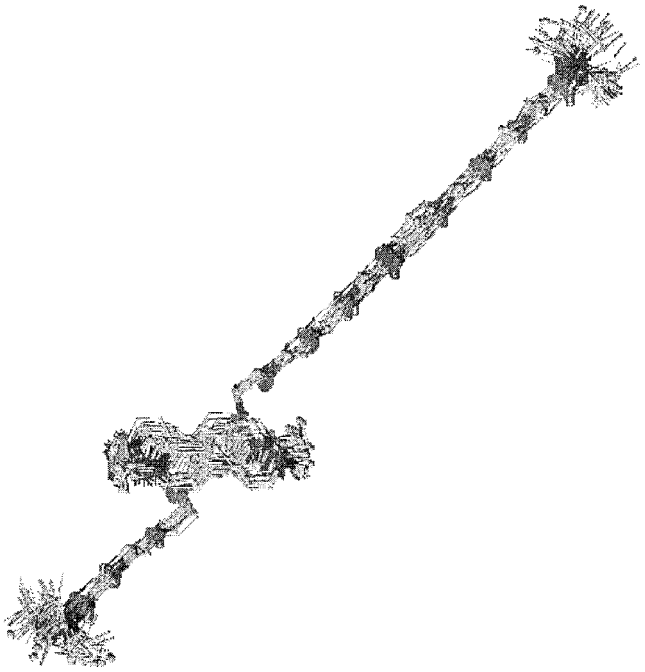

Figure 10. Structures showing the [C−H·····O] hydrogen bond interactions for the global energy minimum (position 6 Å) of [2]rotaxane **1** as obtained in the MD simulations.

can be considered equilibrated (see Figure 8). Curiously, this stabilization coincides with a spreading of the polyether chain, which no longer interacts with the macrocycle through alongside $\pi-\pi$ stacking. However, the [C−H·····O] hydrogen bonding interactions remain intact, denoting a relatively much stronger energy contribution to the total energy. Figure 10 shows the equilibrated structures for the global energy minimum (6 Å, see Figure 5).

Conclusions

The main goal for the future design and synthesis of new [2]rotaxanes, which could act as molecular devices, is to control the positioning of the macrocycle in exclusively one of the two stations, even at thermal equilibrium. The molecular mechanics studies undertaken on this series of [2]rotaxanes have shown that electrostatics and van der Waals terms are the major factors controlling the formation of energy minima. We predict that by altering either of these factors the thermal equilibrium between translational isomers can be modified.

The study of the structure for the cyclobis(paraquat-*p*-phenylene) and the global molecular architecture for the considered [2]rotaxanes has been carried out by molecular mechanics (MM3 and MM3*) calculations. The emulation of the behavior of the [2]rotaxanes as molecular devices at thermal equilibrium using the MM3 force field agrees with the experimental results for the preferred localization of the translational isomers only when ϵ is changed to simulate solvent effects. The same emulation using the MM3* force field shows that this force field has a random and in some cases wrong behavior in the prediction of the stability between the different translational isomers. The use of force fields suitably parametrized, mainly for the positively charged pyridine components, can improve the study based on molecular mechanics calculations for these molecular species.

The introduction of steric hindrances in the polyether chain enhances the energy barrier of shuttling. This aspect could be of interest for the future design of new [2]rotaxanes.

The MD simulations indicate that the shuttling process of **1** presents barriers of around 11 kcal/mol. The computed structures show the existence of T-type interactions between the hydroquinone unit and the macrocycle. Computed distances between hydroquinone units and the macrocycle allow consideration of the existence of $\pi-\pi$ stacking interactions. MD simulations allow detection of [C−H·····O] hydrogen bond interactions along all the shuttling process. Alongside $\pi-\pi$ stacking interactions are of much less importance, as demonstrated by the fact that they are not present in the equilibrated structures. These preliminary MD computations qualitatively agree with the MM calculations in the estimation of the shuttling barrier.

Acknowledgment. Financial support from DGES, Ministerio de Educación y Cultura, Spain (project PB96-1181) is gratefully acknowledged. UAB is thanked for a fellowship to X.G.

JO980400T